

Substituted Azolium Disposition: Examining the Effects of Alkyl Placement on Thermal Properties

Karel Goossens,^{1,*†} Lena Rakers,^{2,†} Tae Joo Shin,³ Roman Honeker,²
Christopher W. Bielawski,^{1,4,5,*} and Frank Glorius^{2,*}

¹ Center for Multidimensional Carbon Materials (CMCM), Institute for Basic Science (IBS),
Ulsan 44919, Republic of Korea

² Organisch-Chemisches Institut, Westfälische Wilhelms-Universität Münster, Corrensstraße
40, 48149 Münster, Germany

³ UNIST Central Research Facilities (UCRF) and School of Natural Science, Ulsan National
Institute of Science and Technology (UNIST), Ulsan 44919, Republic of Korea

⁴ Department of Chemistry, UNIST, Ulsan 44919, Republic of Korea

⁵ Department of Energy Engineering, UNIST, Ulsan 44919, Republic of Korea

* E-mail addresses of the corresponding authors:

karel.cw.goossens@gmail.com

bielawski@unist.ac.kr

glorius@uni-muenster.de

† These authors contributed equally to this work.

Supporting Information

Table of Contents

1. Differential scanning calorimetry (DSC) data	S3
2. Thermogravimetric analysis (TGA) data	S6
3. Synchrotron-based small- to wide-angle X-ray scattering (SWAXS) data	S7

1. Differential scanning calorimetry (DSC) data

Abbreviations used in the figures below: SmA = smectic A phase; Iso = isotropic liquid phase. Tabulated DSC data can be found in Table 1.

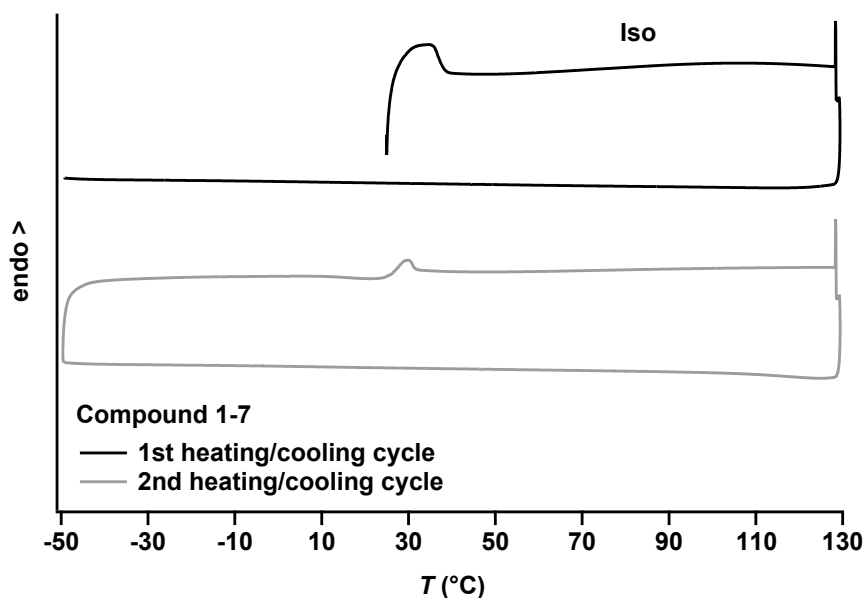


Figure S1. DSC data recorded for compound 1-7 at a heating rate of 10 °C min^{-1} and a cooling rate of 5 °C min^{-1} under an atmosphere of N_2 . Endothermic peaks point upward.

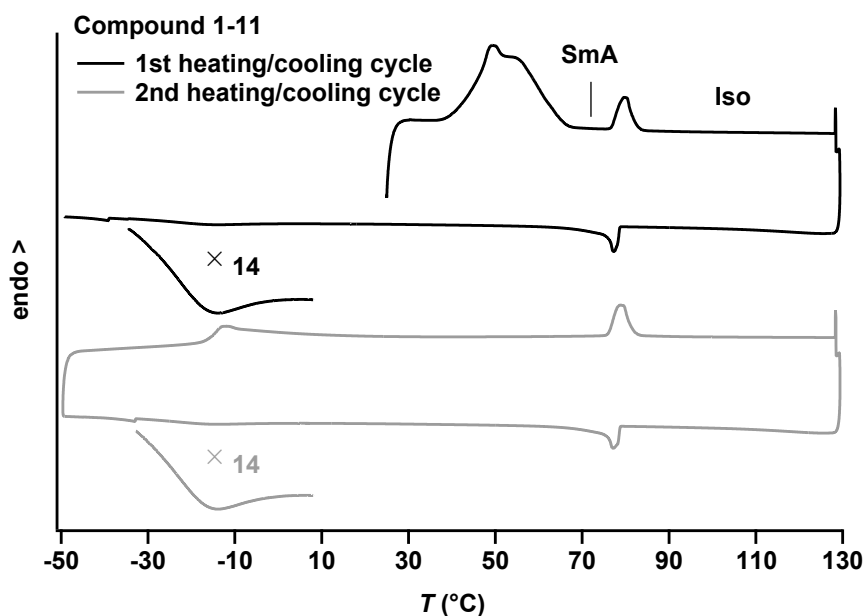


Figure S2. DSC data recorded for compound 1-11 at a heating rate of 10 °C min^{-1} and a cooling rate of 5 °C min^{-1} under an atmosphere of N_2 . Endothermic peaks point upward. The third and fourth heating/cooling cycles were similar to the second heating/cooling cycle.

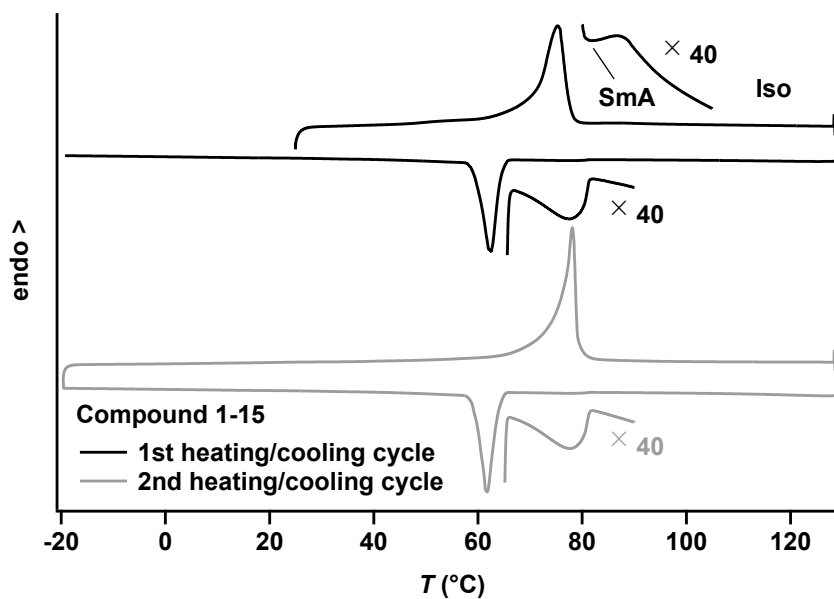


Figure S3. DSC data recorded for compound **1-15** at a heating rate of $10\text{ }^{\circ}\text{C min}^{-1}$ and a cooling rate of $5\text{ }^{\circ}\text{C min}^{-1}$ under an atmosphere of N_2 . Endothermic peaks point upward.

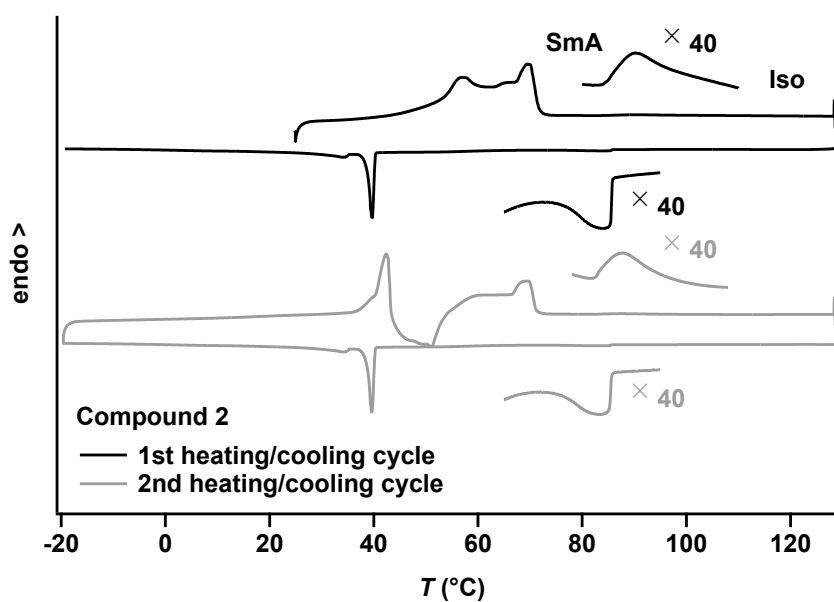


Figure S4. DSC data recorded for compound **2** at a heating rate of $10\text{ }^{\circ}\text{C min}^{-1}$ and a cooling rate of $5\text{ }^{\circ}\text{C min}^{-1}$ under an atmosphere of N_2 . Endothermic peaks point upward.

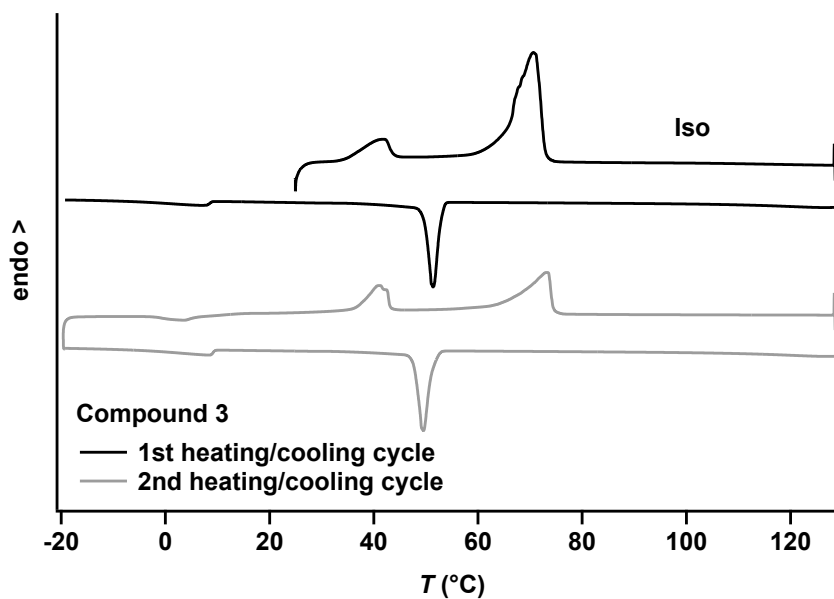


Figure S5. DSC data recorded for compound 3 at a heating rate of $10\text{ }^{\circ}\text{C min}^{-1}$ and a cooling rate of $5\text{ }^{\circ}\text{C min}^{-1}$ under an atmosphere of N_2 . Endothermic peaks point upward.

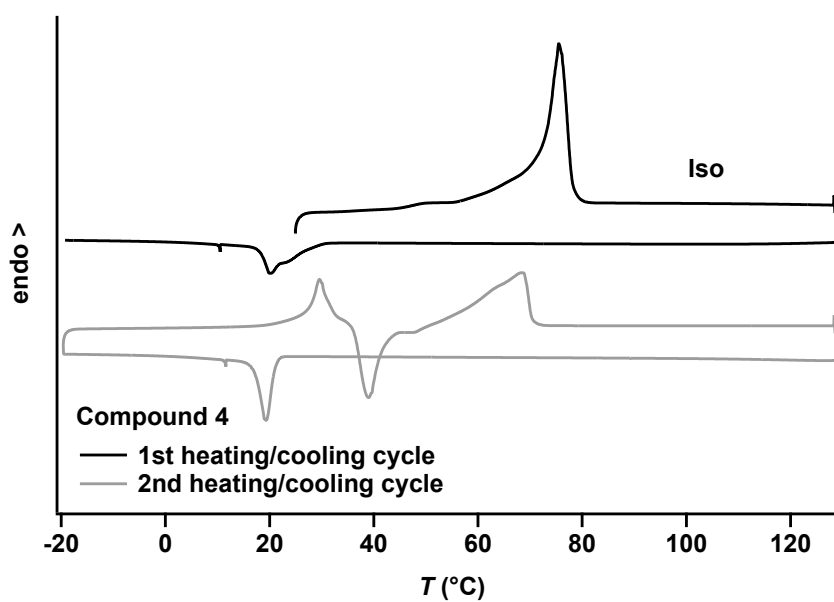


Figure S6. DSC data recorded for compound 4 at a heating rate of $10\text{ }^{\circ}\text{C min}^{-1}$ and a cooling rate of $5\text{ }^{\circ}\text{C min}^{-1}$ under an atmosphere of N_2 . Endothermic peaks point upward.

2. Thermogravimetric analysis (TGA) data

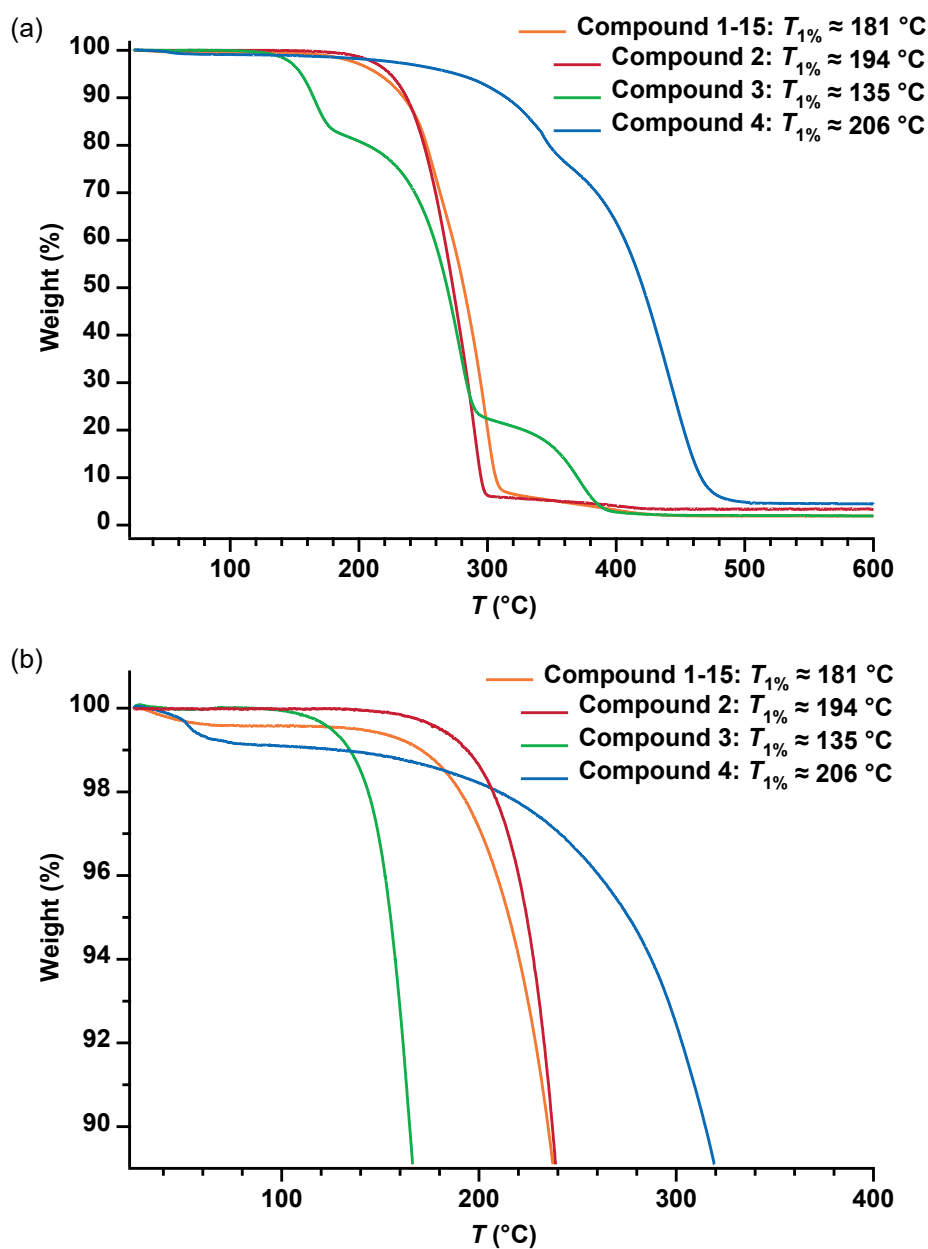


Figure S7. (a) TGA data recorded for compounds **1-15** and **2-4** (heating rate of 5 °C min^{-1} ; N_2 atmosphere). The $T_{1\%}$ value represents the temperature at which 1% weight loss was measured (neglecting the initial small weight loss attributed to the release of H_2O). The observed weight losses for compound **3** are consistent with the expulsion of CH_3I as a first step of decomposition. (b) Enlarged view showing the initial weight losses recorded for compounds **1-15** and **2-4**.

3. Synchrotron-based small- to wide-angle X-ray scattering (SWAXS) data

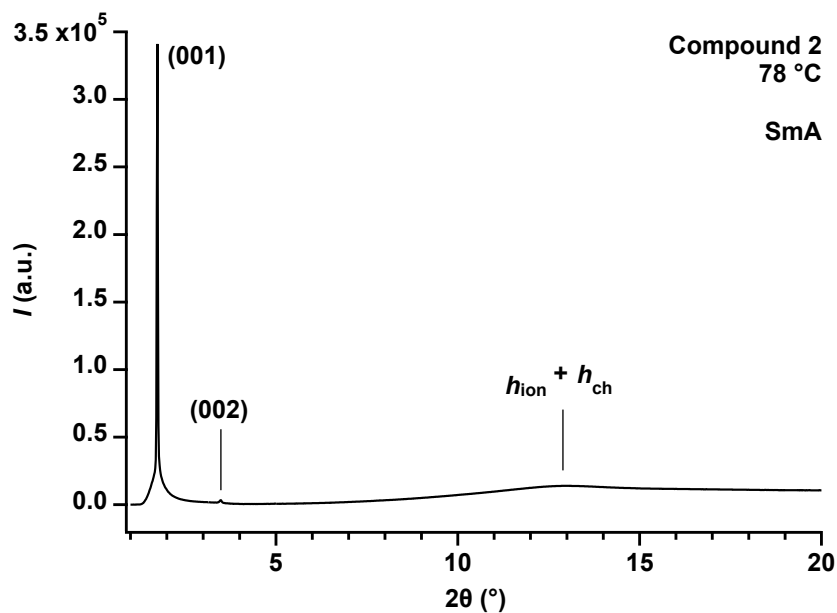


Figure S8. Synchrotron-based SWAXS data that were recorded for the SmA phase of compound 2 at 78 °C (the X-ray wavelength used was 1.00 Å).

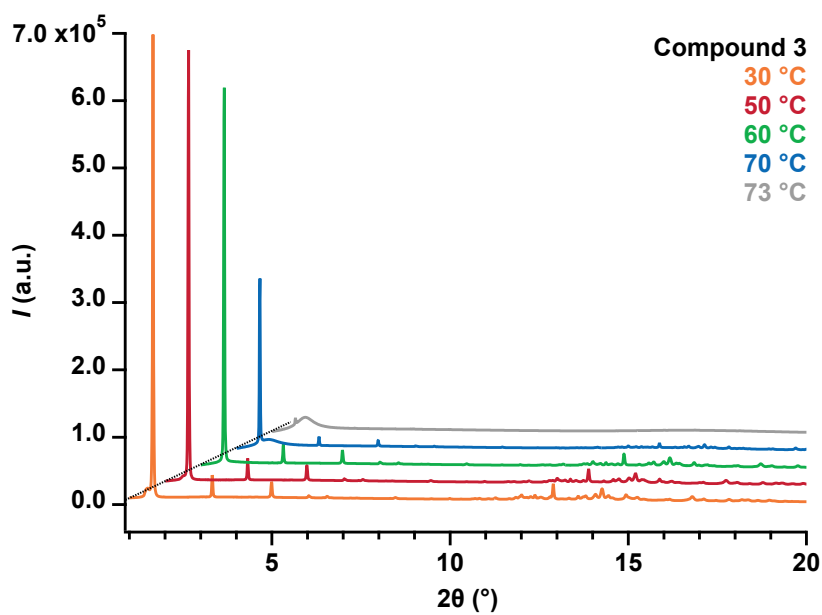


Figure S9. Synchrotron-based SWAXS patterns that were recorded for compound 3 at different temperatures (the X-ray wavelength used was 1.00 Å).